Acta Crystallographica Section F
Structural Biology and Crystallization Communications
ISSN 1744-3091

Crystallization of the extracellular rubber oxygenase RoxA from *Xanthomonas* sp. strain 35Y

Maren Hoffmann,[a] Reinhard Braaz,[b] Dieter Jendrossek[b] and Oliver Einsle[a]*

[a]Abteilung Molekulare Strukturbiologie, Institut für Mikrobiologie und Genetik, Georg-August-Universität Göttingen, Justus-von-Liebig-Weg 11, 37077 Göttingen, Germany, and [b]Institut für Mikrobiologie, Universität Stuttgart, Allmandring 31, 70550 Stuttgart, Germany.

Correspondence e-mail: oeinsle@uni-goettingen.de

Received 19 November 2007
Accepted 11 January 2008

Rubber oxygenase A (RoxA) from *Xanthomonas* sp. strain 35Y is an extracellular dioxygenase that is capable of cleaving the double bonds of poly(*cis*-1,4-isoprene) into short-chain isoprene units with 12-oxo-4,8-dimethyl-trideca-4,8-diene-1-al (ODTD) as the major cleavage product. Crystals of the dihaem *c*-type cytochrome RoxA were grown by sitting-drop vapour diffusion using polyethylene glycol as a precipitant. RoxA crystallized in space group $P2_1$, with unit-cell parameters $a = 72.4$, $b = 97.1$, $c = 101.1$ Å, $\beta = 98.39^\circ$, resulting in two monomers per asymmetric unit. Diffraction data were collected to a limiting resolution of 1.8 Å. Despite a protein weight of 74.1 kDa and only two iron sites per monomer, phasing was successfully carried out by multiple-wavelength anomalous dispersion.

1. Introduction

Natural rubber [poly(*cis*-1,4-isoprene)] is an industrially important biopolymer that is synthesized by various plants and fungi. From the observation that it does not accumulate in nature, the existence of biodegradatory pathways has been inferred. Several rubber-degrading organisms have been identified by their production of clearing zones on natural rubber latex agar; *Xanthomonas* sp. strain 35Y is the only known Gram-negative bacterium among these (Tsuchii & Takeda, 1990). During growth on poly(*cis*-1,4-isoprene), *Xanthomonas* sp. strain 35Y secretes a haem-containing protein, rubber oxygenase A (RoxA), into the medium (Braaz *et al.*, 2004). Purified RoxA was shown to cleave poly(*cis*-1,4-isoprene) *in vitro* by incorporation of oxygen to yield 12-oxo-4,8-dimethyl-trideca-4,8-diene-1-al (ODTD) as the major cleavage product, with a series of related minor byproducts differing only in the number of isoprene units (Braaz *et al.*, 2004; Fig. 1).

The enzyme was first purified as a monomer of 65 ± 7 kDa from the medium of rubber-grown *Xanthomonas* sp. strain 35Y and showed a strong absorption maximum at 406 nm (Braaz *et al.*, 2004). The amino-acid sequence of RoxA comprises two haem-binding motifs Cys-X_1-X_2-Cys-His, which are typical attachment sites for covalently bound haem; RoxA was thus classified as a dihaem *c*-type cytochrome (Jendrossek & Reinhardt, 2003).

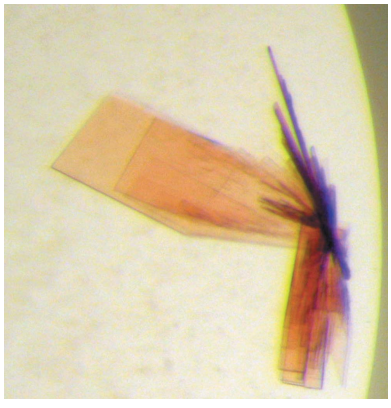

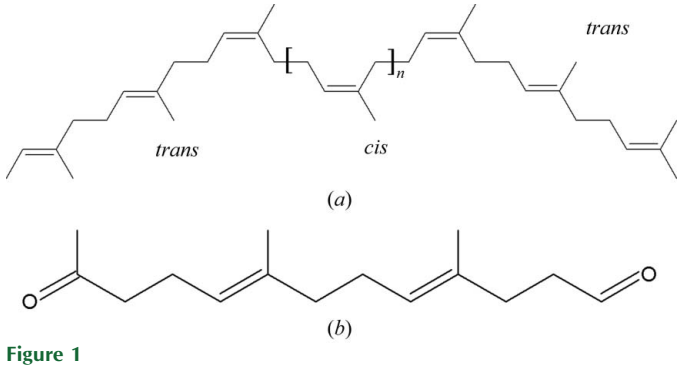

Figure 1
Structure of (*a*) the substrate natural rubber (*cis*-1,4-polyisoprene, $n = 100$–$10\,000$) and (*b*) ODTD (12-oxo-4,8-dimethyl-trideca-4,8-diene-1-al), the main product of rubber cleavage by RoxA.

© 2008 International Union of Crystallography
All rights reserved

Table 1
Data-collection statistics.

Values in parentheses are for the highest resolution shell.

	High resolution	High redundancy	Low remote	Inflection	Peak	High remote
Wavelength (Å)	0.9184	1.7316	1.7711	1.7398	1.7384	1.6754
Energy (eV)	13500	7160	7000	7126	7132	7400
Resolution (Å)	50.0–1.8 (1.78–1.8)	50.0–2.4 (2.4–2.5)	50.0–2.7 (2.8–2.7)	50.0–2.7 (2.8–2.7)	50.0–2.7 (2.8–2.7)	50.0–2.1 (2.2–2.1)
Total reflections	653231	3159992	279358	281548	279523	587171
Unique reflections	126052 (16795)	54970 (5312)	37334 (3189)	37774 (3583)	37788 (3598)	78305 (9065)
Multiplicity	5.1 (4.8)	56.5 (38.6)	7.2 (5.5)	7.2 (6.4)	7.2 (6.4)	7.1 (5.9)
Completeness (%)	98.6 (97.0)	98.3 (92.5)	95.9 (80.1)	97.0 (90.0)	97.0 (90.4)	95.0 (84.7)
$I/\sigma(I)$	10.4 (2.0)	30.2 (6.6)	19.2 (5.9)	22.4 (9.1)	20.6 (8.9)	14.4 (3.4)
$R_{\rm merge}$†	0.106 (0.586)	0.163 (0.633)	0.046 (0.179)	0.037 (0.110)	0.040 (0.113)	0.049 (0.307)
$R_{\rm p.i.m.}$‡	0.051 (0.292)	0.022 (0.096)	0.035 (0.126)	0.028 (0.082)	0.031 (0.085)	0.036 (0.188)

† $R_{\rm merge} = \sum_{hkl}\sum_i |I_i(hkl) - \langle I(hkl)\rangle| / \sum_{hkl}\sum_i I_i(hkl)$. ‡ According to Weiss & Hilgenfeld (1997).

The cleavage of poly(*cis*-1,4-isoprene) by purified RoxA is strictly dependent on the presence of molecular oxygen (Braaz *et al.*, 2004, 2005). To date, the basic molecular mechanism by which poly(*cis*-1,4-isoprene) is degraded is not known. It is assumed that the RoxA-mediated degradation of natural rubber is initiated by the oxidative cleavage of one double bond in the polymer chain.

We have purified RoxA and obtained well diffracting crystals of the oxidized protein using sitting-drop vapour diffusion. A native data set and a high-redundancy data set were collected and a four-wavelength MAD experiment was carried out. Despite the presence of only two Fe atoms per 74.1 kDa monomer of RoxA, taken together these data sets were sufficient to calculate phases that yielded interpretable electron-density maps.

2. Methods

2.1. Cell growth and protein purification

Growth of *Xanthomonas* sp. strain 35Y and purification of the extracellular protein RoxA from the cell-free culture supernatant were performed as described previously (Braaz *et al.*, 2004, 2005). Approximately 5 mg of protein obtained in a single purification were concentrated to 4 mg ml^{-1} by ultrafiltration and exchanged into a buffer containing 5 m*M* Tris–HCl pH 8.5 by size-exclusion chromatography on Sephadex G25.

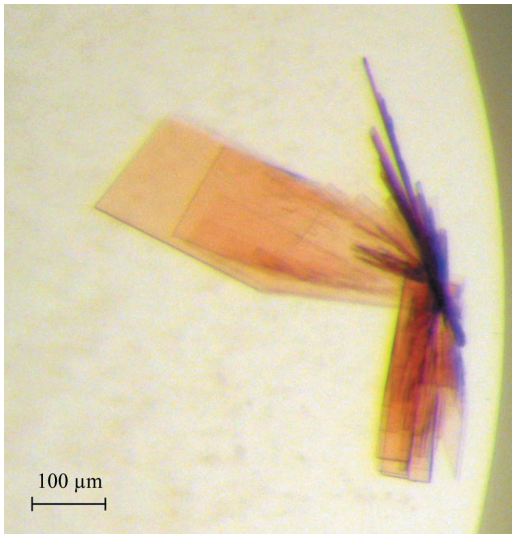

Figure 2
Crystals of RoxA. The rubber oxygenase crystallized in large but thin and fragile plates. Individual plates were separated using accupuncture needles and used for X-ray diffraction experiments.

2.2. Data collection and analysis

Diffraction experiments were carried out on beamline X12 at EMBL/DESY in Hamburg, Germany, on flash-cooled crystals at 100 K. The diffraction images were indexed and integrated with *DENZO* from the *HKL* suite (Otwinowski & Minor, 1997), scaled with the program *SADABS* (Bruker) and analyzed using *XPREP* (Bruker).

3. Results and discussion

3.1. Protein purification and crystallization

The protein was purified to apparent electrophoretic homogeneity (Braaz *et al.*, 2004). Crystals of RoxA were obtained by sitting-drop vapour diffusion at 293 K (Fig. 1). Crystals were grown from a protein solution with a concentration of 4 mg ml^{-1} in a buffer containing 5 m*M* Tris–HCl pH 8.5. Drops consisting of 1 µl protein solution and 1 µl precipitant solution were used in a Cryschem sitting-drop plate (Hampton Research, Laguna Niguel, USA) with a reservoir volume of 300 µl. Initial crystals were obtained using a NeXtal screen (The PEGs; Qiagen, Hilden, Germany) in a condition containing 25%(*w*/*v*) PEG 8000 and 0.1 *M* Tris–HCl buffer pH 8.5. Crystals were optimized in size through manual screening of variations in the PEG concentration, PEG chain length, pH value, buffer substance and additives. In the final optimized crystallization condition, the reservoir contained 500 µl 8%(*w*/*v*) PEG 8000 and 0.1 *M* HEPES–NaOH buffer pH 7.5.

Crystals of RoxA tended to grow in connected stacks or bushels of thin and rather fragile plates (Fig. 2) that had to be separated using microtools or accupuncture needles. For data collection, individual plates were harvested into buffer containing reservoir solution with 10%(*v*/*v*) 2*R*,3*R*-butanediol as a cryoprotectant, mounted in a nylon loop and flash-cooled in liquid nitrogen. The crystals belonged to the monoclinic space group $P2_1$, with unit-cell parameters a = 72.4, b = 97.1, c = 101.1 Å, β = 98.39°. Although they were thin and fragile plates, diffraction data could be recorded to a resolution of 1.8 Å using synchrotron radiation of wavelength 0.9184 Å (Table 1). The theoretical molecular weight of the mature protein derived from the gene sequence is 74.1 kDa. Assuming the presence of two monomers in the asymmetric unit, the solvent content is 48.14%, with a Matthews coefficient $V_{\rm M}$ of 2.37 Å^3 Da^{-1} (Matthews, 1968).

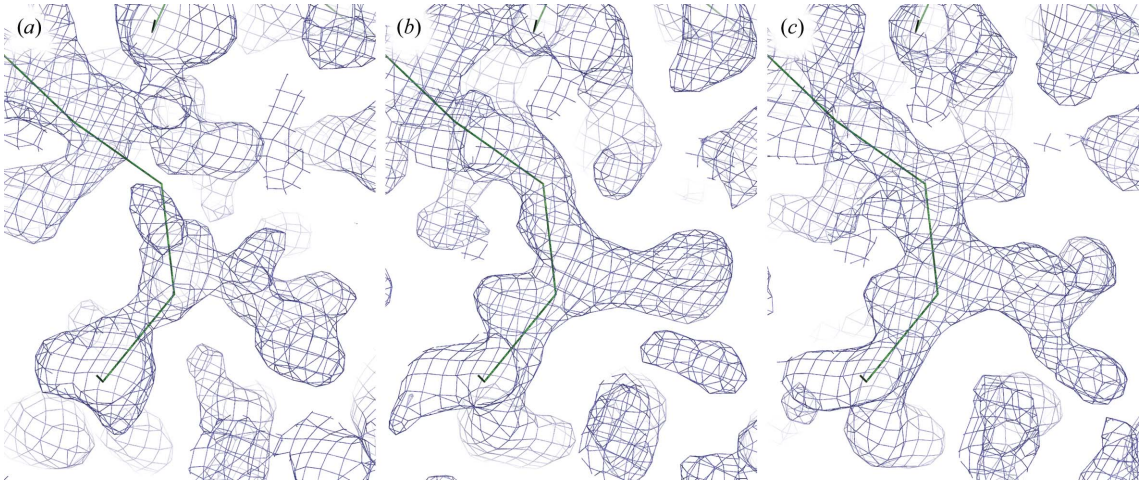

Figure 3
Representative electron density of an identical region of the maps obtained after (*a*) SAD phasing with the high-redundancy data set and the four Fe sites located in the asymmetric unit, (*b*) four-wavelength MAD phasing with four Fe sites and (*c*) combined phasing using both high-redundancy and MAD data, four Fe sites and ten sulfur sites. The trace shows a putative backbone assignment in the ongoing model-building process. All phase calculations were carried out with *SHARP* (de La Fortelle & Bricogne, 1997) and were followed by solvent flattening with *SOLOMON* (Collaborative Computational Project, Number 4, 1994).

3.2. Data collection

Native diffraction data were collected to high resolution (1.68 Å) from a single crystal using synchrotron radiation of wavelength 0.9184 Å. Subsequently, a second data set was collected to a resolution of only 2.4 Å but at an X-ray energy just above the *K* edge of iron and with very high multiplicity (56.5), in order to maximize the quality of the anomalous signal of iron for phasing by single-wavelength anomalous dispersion (SAD). The location of four iron sites per asymmetric unit was straightforward using either *RSPS* (Collaborative Computational Project, Number 4, 1994) or *SHELXD* (Sheldrick, 2008), but the phasing power of two iron sites per 74.1 kDa monomer was insufficient and the resulting electron-density maps were not interpretable. Therefore, a full four-wavelength MAD experiment was carried out in order to obtain additional data for phasing (Table 1). Data sets were recorded at the following wavelengths: low remote at 1.7711 Å, f'' peak at 1.7384 Å, f' inflection at 1.7398 Å and high remote at 1.6754 Å.

3.3. Phase calculations

The four iron sites corresponding to two monomers per asymmetric unit were located with *SHELXD* (Sheldrick, 2008) and used for refinement and phase calculations with *SHARP* (de La Fortelle & Bricogne, 1997). In the first electron-density maps, solvent boundaries could clearly be recognized but interpretation of the maps and model building was still not possible (Figs. 3*a* and 3*b*). However, a total of ten S atoms could be located in anomalous difference Fourier maps and were added in a second run of *SHARP*, resulting in an electron-density map that could not be interpreted by various automatic model-building programs but that was of sufficient quality for manual interpretation (Fig. 3*c*). Seven of the ten S atoms were located close to the Fe atoms at distances that match the expected iron–sulfur distance in a *c*-type haem group covalently linked to the protein chain *via* two cysteine residues.

In summary, the rubber oxygenase RoxA has been crystallized and diffraction data have been collected. This work presents a case of intrinsic iron phasing of a *c*-type cytochrome, albeit with additional information from anomalously scattering S atoms included in order to improve electron-density quality. These sites were located by cross-phasing from a starting set of heavy atoms that only included the four Fe atoms per asymmetric unit. Presently, model building and refinement are under way.

The authors would like to thank Peter Kroneck for stimulating discussions and valuable input on the spectroscopy and function of RoxA. This research was supported by the Deutsche Forschungsgemeinschaft (Ei 520-1/3 to MH and OE, Je 152-7/5 to DJ).

References

Braaz, R., Armbruster, W. & Jendrossek, D. (2005). *Appl. Environ. Microbiol.* **71**, 2473–2478.
Braaz, R., Fischer, P. & Jendrossek, D. (2004). *Appl. Environ. Microbiol.* **70**, 7388–7395.
Collaborative Computational Project, Number 4 (1994). *Acta Cryst.* D**50**, 760–763.
Jendrossek, D. & Reinhardt, S. (2003). *FEMS Microbiol. Lett.* **224**, 61–65.
La Fortelle, E. de & Bricogne, G. (1997). *Methods Enzymol.* **276**, 472–494.
Matthews, B. W. (1968). *J. Mol. Biol.* **33**, 491–497.
Otwinowski, Z. & Minor, W. (1997). *Methods Enzymol.* **276**, 307–326.
Sheldrick, G. M. (2008). *Acta Cryst.* A**64**, 112–122.
Tsuchii, A. & Takeda, K. (1990). *Appl. Environ. Microbiol.* **56**, 269–274.
Weiss, M. S. & Hilgenfeld, R. (1997). *J. Appl. Cryst.* **30**, 203–205.